



## FATIGUE OF RAILWAY STEEL CLIPS

M.F.E. IBRAHIM\*

M.S.GABRA \*\*

\*Dept. of Machine Design, \*\*Dept. of Aeronautical Engineering.  
Military Technical College, Cairo-EGYPT.

## ABSTRACT

Steel clips made from modified 5160H spring steel are used to hold down railway rails to sleepers. The clip has shown fatigue failure, and the cracks are so aligned as to indicate mixed mode loading, i.e. torsion and tension; the latter due to bending.

Specimens has been tested for torsional and push-pull fatigue. Biaxial fatigue theories are used to achieve design conclusions in order to avoid fatigue failure of the clip.

## INTRODUCTION

In many applications the effect of biaxiality of load on cracked components must be investigated because many structures are usually subjected to biaxial or multiaxial stresses. Experiments on the fatigue strength under combined completely reversed bending and torsion were carried out by a limited number of researchers. As a criteria of this loading condition, Gough [1] published the ellipse arc and the ellipse quadrant formulae. Later, ductility effects were specially incorporated in the ellipse correlation of Gough et al [2] by including both torsional ( $t$ ) and bending ( $b$ ) fatigue strengthes. The ellipse quadrant for ductile steels related to the torsional and bending stresses,  $S_t$  and  $S_b$  resp., in a combined bending and torsion test is given by:

$$(S_t/t)^2 + (S_b/b)^2 = 1 \quad (1)$$

\* Dept. of Machine Design, \*\* Dept. of Aeronautical Engineering.  
Military Technical College, Cairo-EGYPT.

Whereas for low ductility cast metals the ellipse arc was recommended as follows:

$$(S_t/t)^2 + (S_b/b)^2 + (b/t - 1) + (S_b/b)(2 - b/t) = 1 \quad (2)$$

Another approach to the problem has been attempted by Brown and Miller [3], to relate the fatigue strength of components subjected to combined stresses to various failure criteria, e.g. Rankine, Tresca, von Mises, St Venant theories ... etc.

Brown [4] suggested that a plot of the maximum shear strain amplitude against the tensile strain amplitude normal to the plane of maximum shear will illustrate the controlling processes in fatigue crack growth at each state of strain.

The two strains mentioned above are represented on Mohr's circle of strain by the highest point of the largest Mohr's circle, see Fig. 1.

The co-ordinates of this point may be derived in terms of the principal strains such that :

$$\frac{\gamma}{2} = \frac{\epsilon_1 - \epsilon_3}{2} \quad (3)$$

where  $\gamma$  is the maximum engineering shear strain, and

$$\epsilon_n = \frac{\epsilon_1 + \epsilon_3}{2} \quad (4)$$

where  $\epsilon_n$  is the tensile strain on plane of maximum shear.

Hence constant life contours can be represented on a graph of  $\gamma/2$  against  $\epsilon_n$  by the equation

$$\frac{\epsilon_1 - \epsilon_2}{2} = f\left\{ \frac{\epsilon_1 + \epsilon_3}{2} \right\} \quad (5)$$

where  $\epsilon_1 \geq \epsilon_2 \geq \epsilon_3$

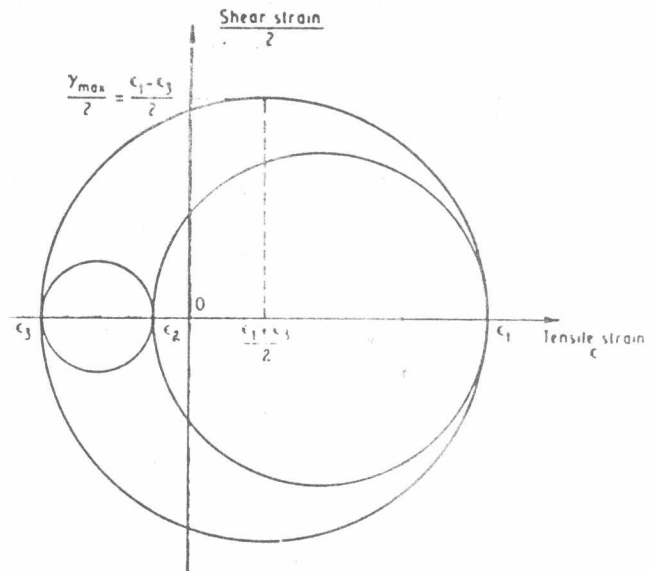


Fig. 1. Mohr's circle of strain



Henceforward, the graph of maximum shear strain,  $\gamma/2$ , against the tensile strain,  $\epsilon_n$ , normal to the maximum shear strain plane is known as the  $\Gamma$ -plane, and the contours of constant endurance are called as the  $\Gamma$ -plots. Thus each  $\Gamma$ -plot is associated with a given life.

In Fig.2 graphs are plotted for Poisson's ratio of  $\frac{1}{2}$  and  $\frac{1}{3}$  in terms of  $\epsilon_n$  and  $\frac{1}{2} \gamma_{max}$ , on which four various failure criteria are represented by different loci, for a biaxial stress state.

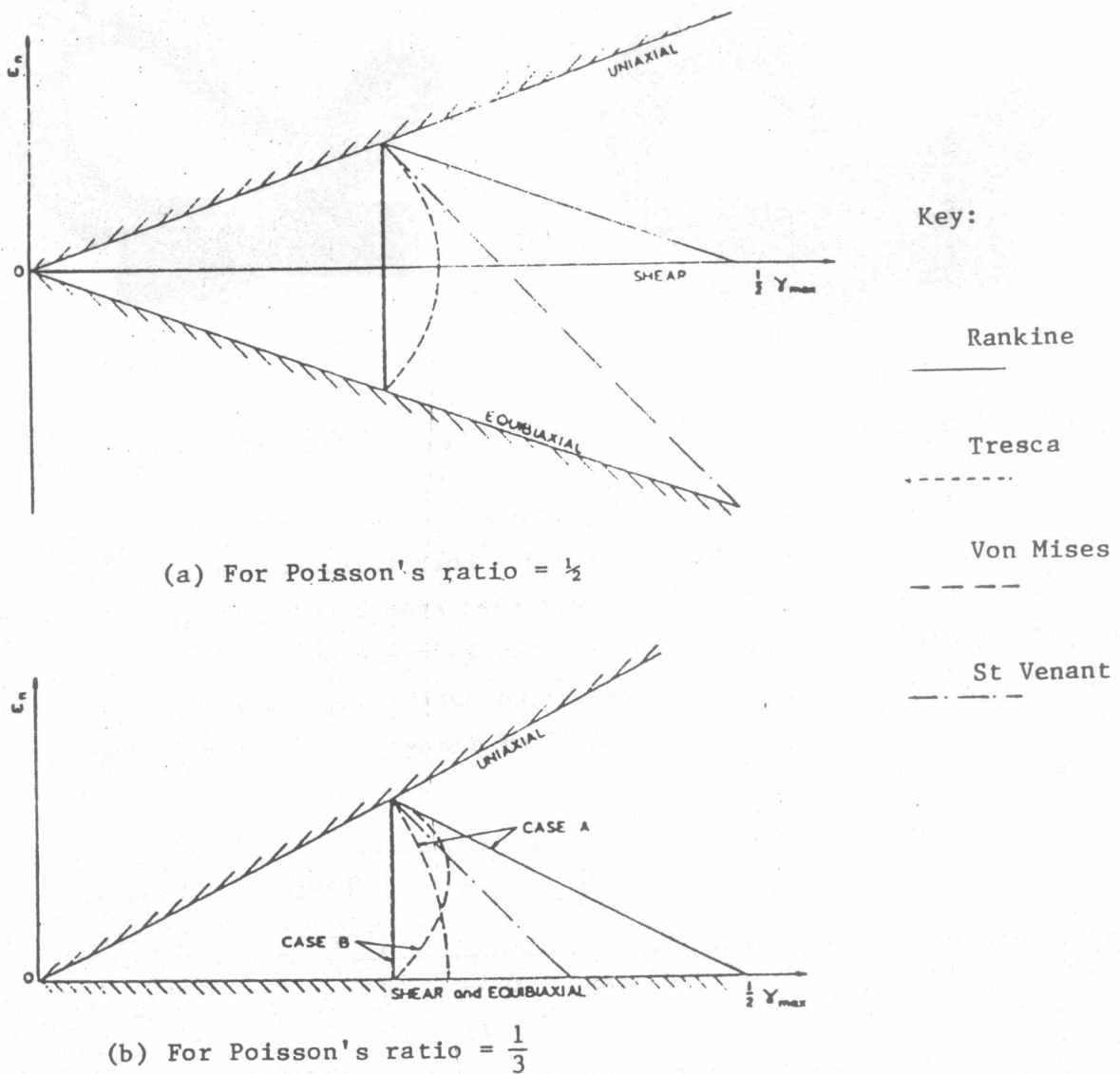
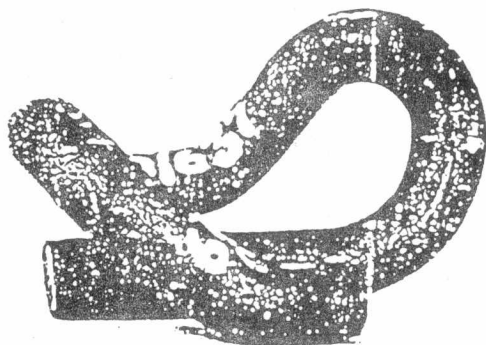


Fig.2. Classical Failure Critereria on the  $\Gamma$ -plane



DESCRIPTION OF THE PROBLEM

Figure 3 shows the steel clip that holds down railway rails to sleepers. This clip has shown signs of fatigue, see Fig.4. The cracks are so aligned as to indicate mixed mode loading, i.e. torsion and tension the latter due to bending.



$\frac{1}{\text{cm}}$

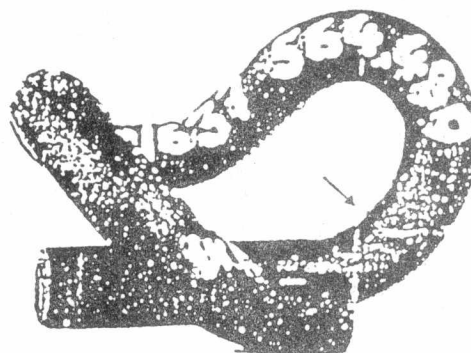


Fig. 3. The Steel Clip.

Fig.4. Fatigue Crack.

A preliminary examination of directions of loading suggested that the crack was initiated by shear loading due both torsional, and bending forces giving Stage I growth, and was then propagated in Stage II due to mainly uniaxial loading, i.e. Mode I crack development.

The material tested was a modified 5160H spring steel which was supplied in the form of hot pressed bars 22.25 mm diameter, with the following composition and heat treatment.

C	Si	Mn	P + S	C <sub>r</sub>	Quen. (oil)	Temp. (1 hr)
0.55-	0.8-	0.75-	0.05 max	0.4-	870°C	525°C
0.65	1.1	1.0		0.6		

The mechanical properties of this steel are as follows:

0.2% proof stress	= 1277.24	MPa
Ultimate tensile strength	= 1408.52	MPa
Percentage elongation	= 11	

Percentage reduction in area	= 47
Impact	= 18 Joules
Grain size	ASTM 5-8

#### EXPERIMENTAL STUDY

Figure 5 shows the detailed dimensions of the fatigue test specimen cut from the 22.25 mm bars. The specimens were finished by polishing alternatively in longitudinal, helical and circumferential directions with successively finer grades of emery paper, the final polishing being done with grade 4/0 paper circumferentially. They were then carefully inspected under a microscope to ensure that no serious scratches remained. Random measurement of surface roughness of three specimens showed that the maximum CLA was 0.1  $\mu\text{m}$ .

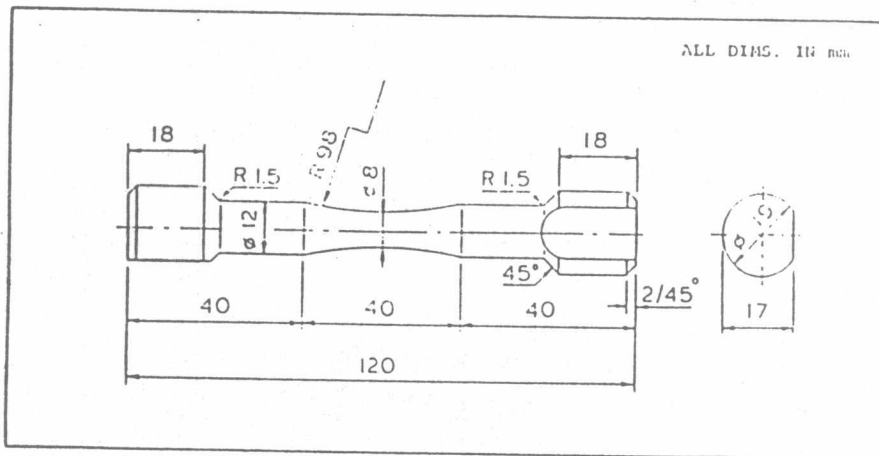


Fig.5. Specimen Geometry.

#### Torsion Fatigue Test:

The torsion fatigue properties were produced from the testing of 10 specimens. Cyclic torsion was carried out under constant strain limits controlled by the applied angle of twist  $\Delta\theta$ .

A record of torque against angle of twist obtained from a multiple step test at different strain levels produced on one specimen is shown in Fig. 6. The cyclic stress-strain curve, shown in Fig. 7. was also derived for the 5160H spring steel specimens.

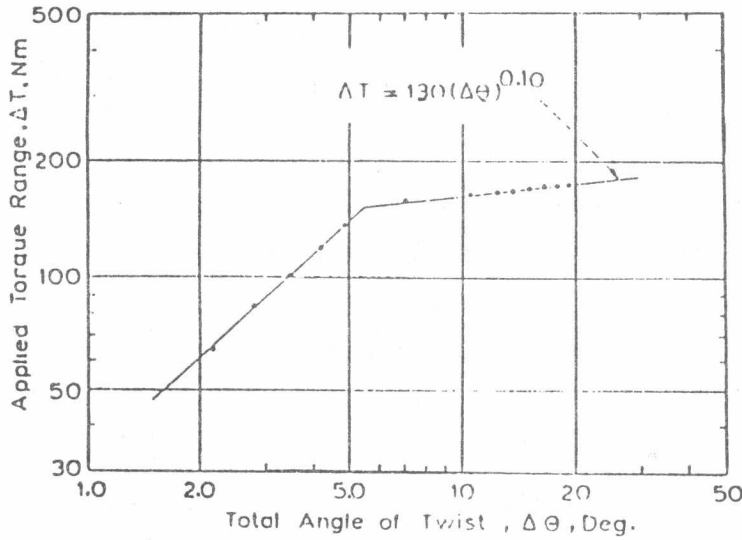
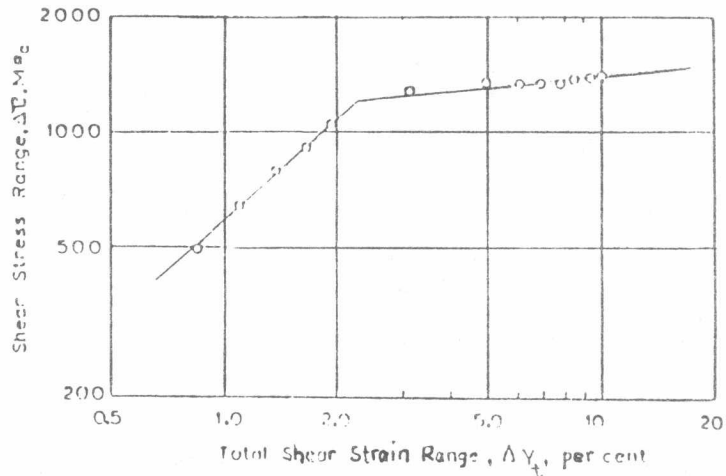


Fig. 6. Torque vs Twist characteristic.

Fig. 7. Shear stress vs shearstrain characteristic.



The fatigue test results are tabulated in Table I, and plotted in Fig. 8. The  $\Delta\sigma$  vs  $N_f$  curve does not exhibit a clearly discernable break within the performed range of tests. Considering the fatigue strength corresponding to 10 million cycles as a convenient base for design , the fatigue strength may be taken as equal to  $\pm$  300 MPa.



Table I Torsion Fatigue Test

Spec. No.	Min. Diam. d	Total Angle of Twist $\Delta\theta$	Applied Torque $\Delta T$	Shear Stress $\Delta\tau$	Shear Strain $\Delta\gamma_t$	No. of Cycles to Failure $N_f$
	mm	Deg.	Nm	MPa	%	Cycles
1	8.040	13.90	165.10	1262.22	7.09	160
2	7.980	9.26	158.14	1235.91	4.43	590
3	7.925	7.66	142.94	1140.49	3.51	920
4	8.040	5.40	134.17	1025.27	2.26	4952
5	8.020	3.80	111.81	860.80	1.51	33809
6	7.890	3.50	100.63	797.15	1.39	75024
7	8.040	3.20	96.90	725.46	1.27	221353
8	8.030	3.00	92.43	694.57	1.19	768721
9	8.030	2.80	85.72	644.16	1.11	3573275
10	7.890	2.20	67.83	548.46	0.88	$1.65 \times 10^7$ *

\* Unbroken

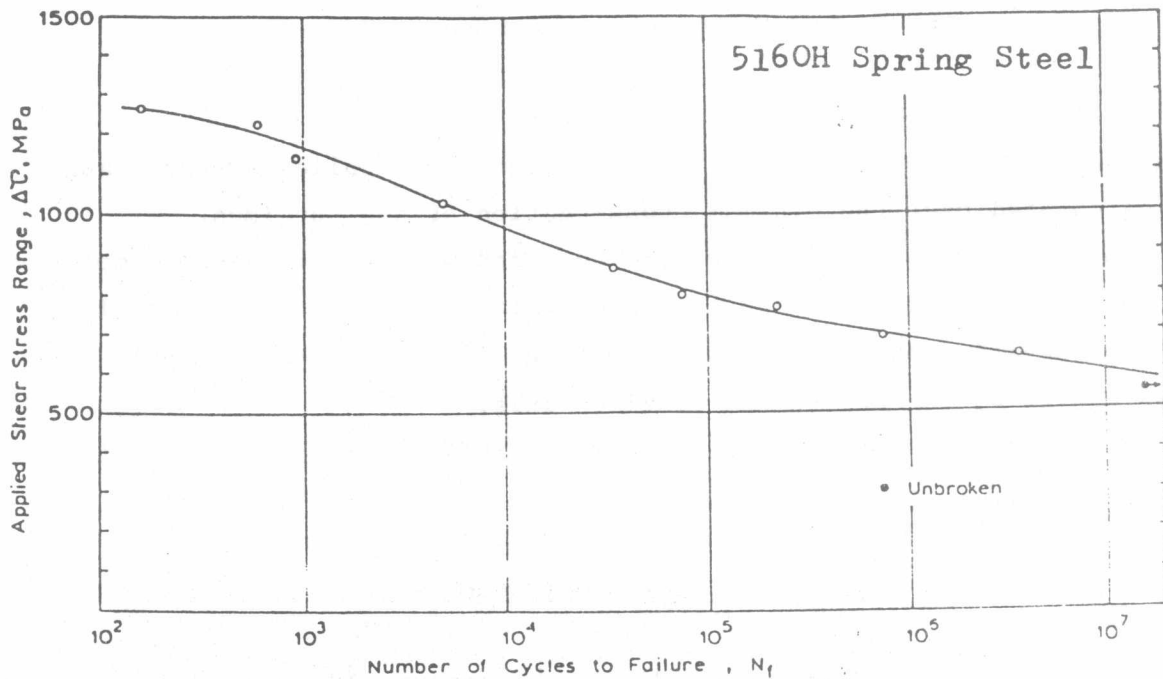


Fig.8 . Torsional Fatigue Endurance Behaviour.

Push-Pull Fatigue Test:

Another 10 specimens with the same geometry were fatigue tested under push-pull cycling with zero mean stress. The test was carried under stress control conditions. It was difficult to record the corresponding strain values because the transducer failed to clip on the extremely hard test specimen. However, the stress-strain cyclic behaviour was calculated

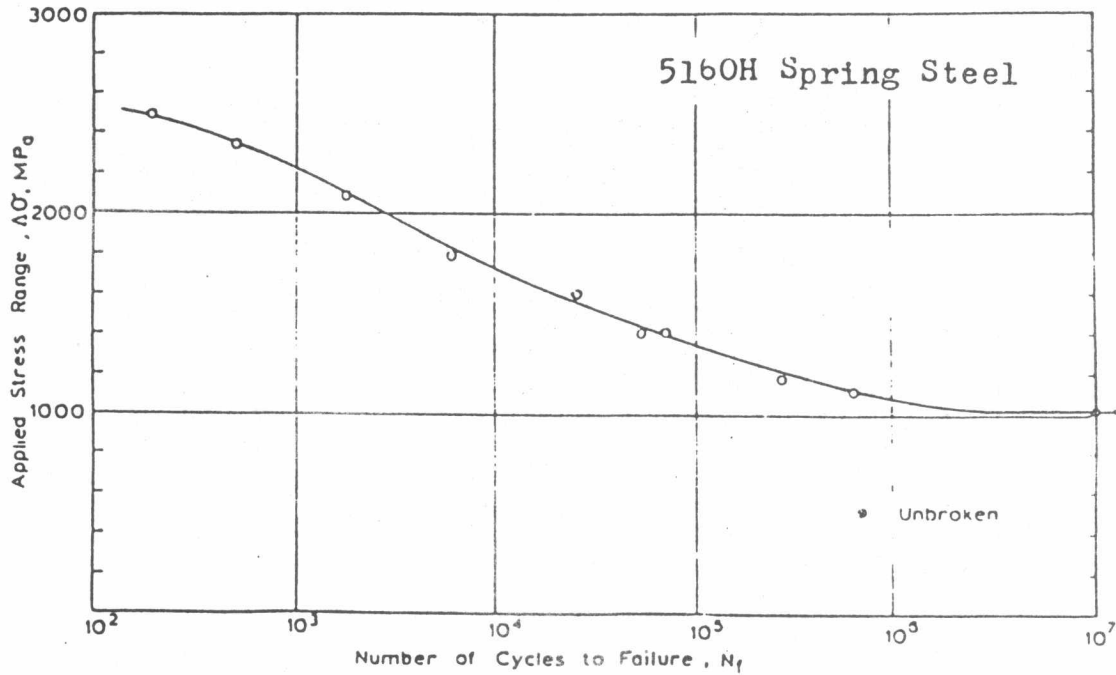


Fig.9. Push-Pull Fatigue Endurance Behaviour.

from that obtained in torsion, Fig. 7 |5|. The applied stress range was calculated over the minimum cross-section of the specimen. The number of cycles to failure were recorded when the specimen completely fractured. Observation of the fracture surfaces revealed that the slow crack propagation stage was typically Stage II whereas the unstable growth stage was at 45 degrees to the specimen axis. The fatigue test results are tabulated in Table II and plotted in Fig.9, giving a fatigue limit at  $\pm$  510 MPa.

Table II Push-Pull Fatigue Test

Spec. No.	Min. Diam. d	Applied Load $\Delta P$	Stress Range $\Delta\sigma$	No. of Cycles to Failure $N_f$
	mm	KN	MPa	
1	7.820	119.8	2494.33	194
2	7.820	112.0	2331.93	502
3	7.810	100.0	2087.41	1819
4	7.920	88.0	1786.25	6143
5	7.970	80.0	1600.00	25327
6	7.930	69.7	1411.23	53440
7	7.940	70.0	1413.73	60360
8	7.915	58.0	1178.79	275156
9	7.870	54.3	1116.25	636239
10	7.950	50.5	1017.34	$10^7$

• Unbroken



### BIAXIAL FATIGUE LIMIT PREDICTION

In order to predict the fatigue limit under combined bending and torsional stress the "Gough" ellipse quadrant is suggested which is described by equation (1) .

The experimental data obtained under push-pull and torsion cyclic loading indicate via Figures 8 and 9 that

- (i) the uniaxial fatigue strength  $b = \pm 510$  MPa.
- (ii) the torsional fatigue strength  $t = \pm 300$  MPa.

Substituting these values in equation (1) gives the predicted fatigue strength under biaxial loading situations, Point A, Fig. 10.

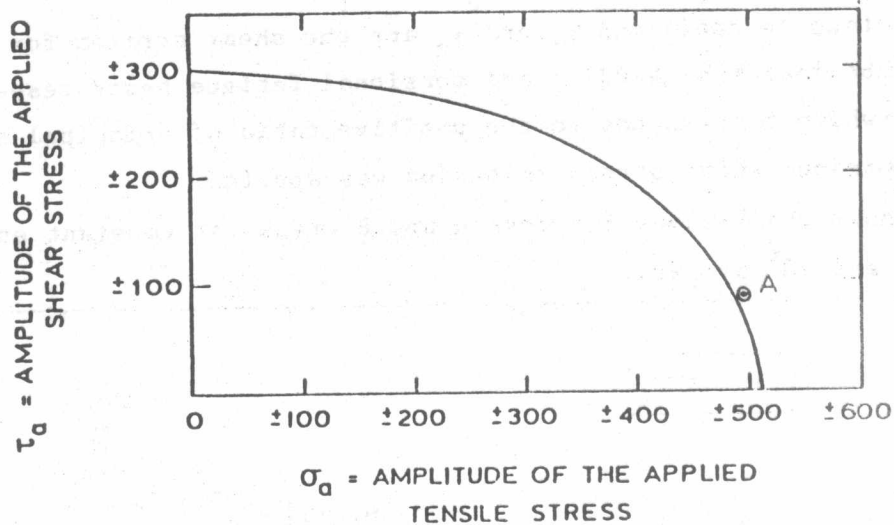


Fig.10. Gough Ellipse Quadrant for Biaxial Fatigue Limit Prediction.



## CONTOURS OF CONSTANT ENDURANCE

Fatigue life is controlled by the maximum shear strain,  $\gamma_{\max}$ , and the normal strain on that plane of maximum shear  $\epsilon_n$ , or simply.

$$N_f = f(\gamma_{\max}, \epsilon_n) \quad (6)$$

Two types of fatigue cracks, labelled as cases A and B [6], may result corresponding to the orientation of the free surface with respect to the axes of principal strain. Contours of constant endurance for case A and case B fatigue cracks are usually presented on a graph of  $\frac{1}{2} \gamma_{\max}$  vs  $\epsilon_n$ , which is termed a  $\Gamma$ -plane.

For the derivation of the formulae representing the contours of constant endurance for case A cracks equation (1) was converted into strain terms to give the following format:

$$\left(\frac{\gamma_{\max}}{\gamma_t}\right)^2 + 4\left(\frac{1+\nu}{1-\nu}\right)^2 \left(\frac{1}{\gamma_b^2} - \frac{1}{\gamma_t^2}\right) \epsilon_n^2 = 1 \quad (7)$$

where  $\nu$  is poisson's ratio and  $\gamma_b$  and  $\gamma_t$  are the shear strains for a given life obtained from bending and torsional fatigue tests respectively. For case B, which corresponds to the positive ratio of principal stresses  $\sigma_2/\sigma_1$ , the maximum shear stress criterion was applied.

Figure 11 shows the  $\Gamma$ -plane for case A and B cracks at constant endurance of  $10^4$ ,  $10^5$  and  $10^6$  cycles.

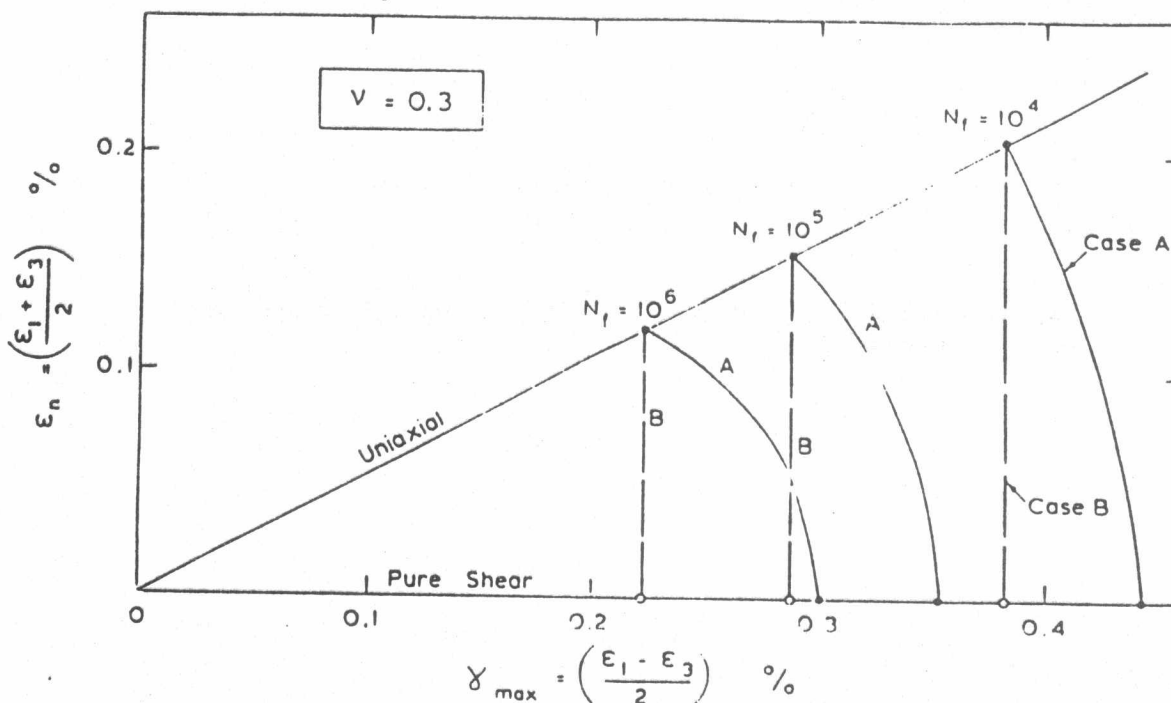


Fig.11.  $\Gamma$ -Plane and Fatigue Life Contours for Biaxial Fatigue Behaviour.

### CONCLUSIONS

1. A Gough quadrant equation has been derived for the steel clip, subjected to combined bending and torsion that induce applied tensile and shear stresses, namely for an endurance of  $10^7$  cycles.
2. From the orientation of the crack ( $10^\circ$  from the transverse plane of the bar) it can be assumed from Mohr's circle of stress that the values of  $\sigma_a$  and  $\tau_a$  are 496 MPa and 89 MPa, respectively, (see Fig. 12).  
When comparing this result with "Gough" ellipse, as indicated by point A in Fig. 10, shows that Gough predictions for failure under biaxial loading is safer.
3. In order to reduce the possibility of fatigue the maximum principal stress should be reduced, critical crack size increased and the surface finish improved.

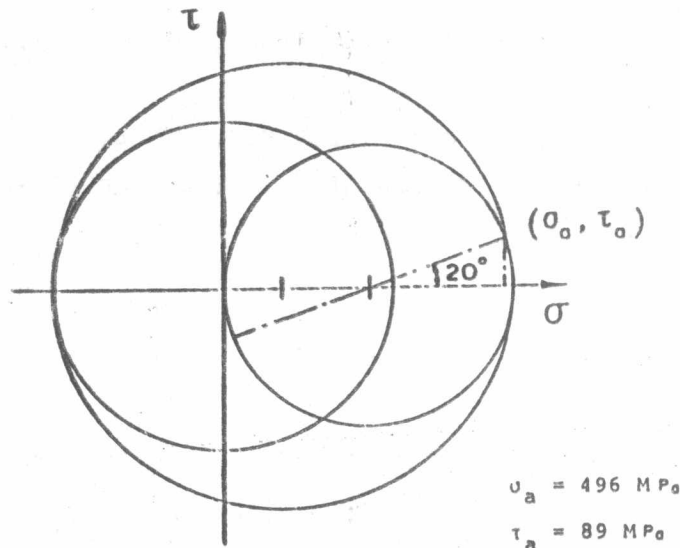


Fig.12. Mohr's Stress Circle.

### ACKNOWLEDGEMENT

The Authors are very grateful to Prof. K.J. Miller, Head of the Mechanical Engineering Department, Sheffield University for his encouragement and valuable suggestions. Thanks to Pandrol Claylands Forge for supply of the steel.



REFERENCES

- [1] GOUGH, H.J. and POLLARD, H.V., 1935,  
'The strength of metals under combined alternating stresses', Proc. Instn. Me ch. Engrs. Vol. 131.
- [2] GOUGH, H.J., POLLARD, H.V. and  
CLENSHAW, W.J., 1951, "Some experiments on the resistance of metals to fatigue under combined stress", Aero. Res Council Rep. Memos 2522.
- [3] BROWN, M.W. and MILLER, K.J., 1973,  
' A theory for fatigue failure under multi-axial stress-strain conditions', Proc. Instn. Mech. Engrs. Vol. 187.
- [4] BROWN, M.W. and MILLER, K.J., 1979,  
'Initiation and Growth of cracks in biaxial fatigue', Fatigue Engng. Mat. Struct . Vol. 1.
- [5] IBRAHIM, M.F.E., 1981,  
' Early damage accumulation in metal fatigue', Ph. D. Thesis. Sheffield University.
- [6] IBRAHIM , M.F.E, HAMMOUA, M.M.I. and MILLER, K.J., 1984,  
'Mixed mode cumulative fatigue damage' Proc. First AME confr. MTC CAIRO, Vol. 1